

## Identification of senescence and death in *Emiliania huxleyi* and *Thalassiosira pseudonana*: Cell staining, chlorophyll alterations, and dimethylsulfoniopropionate (DMSP) metabolism

Daniel J. Franklin,<sup>a,b,\*</sup> Ruth L. Airs,<sup>c</sup> Michelle Fernandes,<sup>b</sup> Thomas G. Bell,<sup>b</sup> Roy J. Bongaerts,<sup>d</sup> John A. Berges,<sup>e</sup> and Gill Malin<sup>b</sup>

<sup>a</sup>School of Applied Sciences, Bournemouth University, Talbot Campus, Fern Barrow, Poole, United Kingdom

<sup>b</sup>Laboratory for Global Marine and Atmospheric Chemistry, School of Environmental Sciences, University of East Anglia, Norwich, United Kingdom

<sup>c</sup>Plymouth Marine Laboratory, Prospect Place, Plymouth, United Kingdom

<sup>d</sup>Institute of Food Research, Norwich Research Park, Norwich, United Kingdom

<sup>e</sup>Department of Biological Sciences, University of Wisconsin-Milwaukee, Milwaukee, Wisconsin

### Abstract

We measured membrane permeability, hydrolytic enzyme, and caspase-like activities using fluorescent cell stains to document changes caused by nutrient exhaustion in the coccolithophore *Emiliania huxleyi* and the diatom *Thalassiosira pseudonana*, during batch-culture nutrient limitation. We related these changes to cell death, pigment alteration, and concentrations of dimethylsulfide (DMS) and dimethylsulfoniopropionate (DMSP) to assess the transformation of these compounds as cell physiological condition changes. *E. huxleyi* persisted for 1 month in stationary phase; in contrast, *T. pseudonana* cells rapidly declined within 10 d of nutrient depletion. *T. pseudonana* progressively lost membrane integrity and the ability to metabolize 5-chloromethylfluorescein diacetate (CMFDA; hydrolytic activity), whereas *E. huxleyi* developed two distinct CMFDA populations and retained membrane integrity (SYTOX Green). Caspase-like activity appeared higher in *E. huxleyi* than in *T. pseudonana* during the post-growth phase, despite a lack of apparent mortality and cell lysis. Photosynthetic pigment degradation and transformation occurred in both species after growth; chlorophyll *a* (Chl *a*) degradation was characterized by an increase in the ratio of methoxy Chl *a*: Chl *a* in *T. pseudonana* but not in *E. huxleyi*, and the increase in this ratio preceded loss of membrane integrity. Total DMSP declined in *T. pseudonana* during cell death and DMS increased. In contrast, and in the absence of cell death, total DMSP and DMS increased in *E. huxleyi*. Our data show a novel chlorophyll alteration product associated with *T. pseudonana* death, suggesting a promising approach to discriminate nonviable cells in nature.

Phytoplankton cell physiology is fundamental to global biogeochemical cycles because the mediation of biogeochemical processes by phytoplankton, such as the production of the trace gas dimethylsulfide and carbon fixation, strongly depends on cell physiological state. Nondividing alternative physiological states include senescence, quiescence (dormancy), and death (Franklin et al. 2006). Such alternative states are poorly understood, especially in eukaryotic marine phytoplankton, but are likely to be significant in natural assemblages. Some progress has been made in recognizing cell state in the laboratory: the morphological changes associated with nutrient limitation in batch cultures have been studied, and similarities with metazoan programmed cell death (PCD; Bidle and Falkowski 2004; Franklin et al. 2006) have been described in certain phytoplankton (e.g., *Dunaliella tertiolecta*; Segovia and Berges 2009). An improved ability to recognize senescent, quiescent, moribund, and dead cells within microbial populations is important because a substantial fraction of natural phytoplankton biomass may be nonviable (Veldhuis et al. 2001; Agustí 2004) and yet viability will be a major driver of primary production and biogeochemistry. Accurate estimation of phytoplankton primary production through remote sensing could be improved by

practical recognition of different physiological states. Although efforts to understand physiological change in terms of variable pigment content within photosynthesizing cells via remote sensing (Behrenfeld and Boss 2006) offer a useful way to assess natural physiological variability, the ability to discriminate “viability” cannot currently be achieved by remote sensing. In order to achieve this, we need to find robust indicators of cell death that have value in the field. As part of this effort we undertook a laboratory study that aimed to provide tools for field assessments of phytoplankton viability.

Chlorophyll *a* (Chl *a*) alteration during senescence is of great interest in organic geochemistry (Louda et al. 2002; Szymczak-Zyla et al. 2008) and may be useful as a field signal of phytoplankton cell death. One potential difficulty is that observations of Chl *a* alteration have not been explicitly linked with microalgal growth phase or physiological state (Louda et al. 2002), limiting its usefulness as an indicator of cell death. In general, increased concentrations of chlorophyll oxidation products have been observed in nutrient-depleted cells, but it is likely that specific chlorophyll transformation pathways vary between species (Bale 2010). Initial investigations into pigment alteration and cell viability in natural phytoplankton assemblages (using SYTOX Green staining) have used pigment fluorescence to assess chlorophyll loss (Veldhuis et al. 2001). Such

\* Corresponding author: dfranklin@bmath.ac.uk

approaches have been useful, but miss vital information on the early alteration of chlorophyll. Early alteration mostly gives structures with indistinguishable absorption and fluorescence properties from the parent compound and which are, therefore, invisible to fluorescence-based methods. Molecular structures resulting from early stage alterations can be produced by the reaction of Chl *a* with, for example, the reactive oxygen species H<sub>2</sub>O<sub>2</sub> (Walker et al. 2002), and likely occur in conjunction with cell death because reactive oxygen species are associated with cell death. High-performance liquid chromatography (HPLC) methods vary in their ability to separate and detect chlorophyll allomers (Airs et al. 2001), and a suitable method has not yet been applied to the model species of this study in combination with independent measures of cell viability. In our study we link an assessment of viability (using flow cytometry) with a high-resolution HPLC method (Airs et al. 2001), in combination with liquid chromatography–mass spectrometry (LC-MS) characterization, in order to assess the pigment changes associated with changing physiological state.

Dimethylsulfide (DMS) is the main natural source of reduced sulfur to the troposphere (Simó 2001). DMS is a volatile trace gas that promotes aerosol formation and thereby affects global climate (Charlson et al. 1987). The molecular precursor of DMS, the compatible solute dimethylsulfoniopropionate (DMSP), occurs at high intracellular concentrations (100–400 mmol L<sup>-1</sup>) in coccolithophores such as *Emiliania huxleyi* (Keller et al. 1989), and at lower concentrations in diatoms (Keller and Korjef-Bellows 1996). DMSP can be released to the seawater dissolved organic carbon pool through grazing, viral lysis, cell senescence, or active exudation, but information on the latter two processes is very limited (Stefels et al. 2007). Intracellular DMSP concentration increases in some phytoplankton species when growth is limited due to CO<sub>2</sub> or iron (Fe) limitation, ultraviolet light exposure, toxic levels of cupric ions, or addition of hydrogen peroxide (Sunda et al. 2002). On this basis, Sunda et al. (2002) suggested that DMSP and its lysis products DMS and acrylate may form an antioxidant cascade. This would presumably increase the survival of phytoplankton cells during conditions associated with oxidative stress and elevated levels of reactive oxygen species. An alternative hypothesis is that under conditions of unbalanced growth an overflow mechanism operates whereby excess energy and reduced compounds are used for DMSP production to ensure the continuation of other metabolic pathways (Stefels 2000). Several studies have shown that nitrogen limitation leads to increased DMSP concentration (Stefels et al. 2007). For example, Harada et al. (2009) recently found that intracellular DMSP concentration increased from 2.1 to 15 mmol L<sup>-1</sup> in 60 h when the diatom *Thalassiosira oceanica* was grown in low-nitrate medium, and this was especially notable when the cells reached the stationary phase. In addition, Archer et al. (2010) showed that under conditions of acute photooxidative stress *E. huxleyi* rapidly accumulated DMSP to a level that was 21% above that of control cells. Such processes must require an intact and functioning metabolism, and a logical next step

is to assess DMSP and DMS production in parallel with assessments of pigments and cell viability.

*E. huxleyi* and *Thalassiosira pseudonana* are good model species for the major calcifying and silicifying phytoplankton groups and are therefore highly relevant for an investigation into cell physiology and its relationship with biogeochemical processes. We grew cells through the batch cycle and used flow cytometry to examine changes in physiological state using fluorescent cell stains for membrane permeability and enzyme activity. In conjunction with these cell viability assays, we investigated the time course of pigment alteration using a high-resolution HPLC-LC-MS method that allows the separation and detection of chlorophyll allomers (Airs et al. 2001). In addition, we analyzed for DMSP and DMS to address the knowledge gap on the production of these compounds relative to cell viability.

## Methods

*Cell culture and growth measurements*—Unialgal duplicate cultures of *E. huxleyi* (CCMP 1516; calcifying) and *T. pseudonana* (CCMP 1335) were grown in 500 mL of ESAW/5 media (enriched seawater, artificial water; Harrison et al. 1980) in 1000-mL borosilicate conical flasks. Silica was omitted in *E. huxleyi* media. Photosynthetically active radiation was supplied at 100 μmol photons m<sup>-2</sup> s<sup>-1</sup> (Biospherical Instruments QSL 2101) from cool white fluorescent tubes, on a 14:10 h light:dark cycle (08:00 h to 22:00 h) at a constant temperature of 17°C. Each day at the same time (10:00 h) biomass was quantified as cell number, cell (or coccusphere in the case of *E. huxleyi*) volume (Beckman Coulter MS3), and fluorescence (Heinz-Walz GmbH; PHYTO-PAM equipped with a PHYTO-ED measuring head). The efficiency of Photosystem II (F<sub>V</sub>:F<sub>M</sub>; 30-min dark acclimation) was measured at the same time.

*Flow cytometry and cell staining*—Fluorescent staining analyses were conducted with three molecular probes. Two of these have been described as “live” and “dead” stains; SYTOX Green can be used to measure changes in membrane permeability (Veldhuis et al. 1997; “dead” cells) and 5-chloromethylfluorescein diacetate (CMFDA) is cleaved by a variety of enzymes, indicating hydrolytic enzymatic activity (D. J. Franklin and J. A. Berges unpubl. data; Garvey et al. 2007; “live” cells). SYTOX Green (Invitrogen S7020) was applied at a final concentration of 0.5 μmol L<sup>-1</sup> during a 10-min culture-temperature dark incubation. Uptake of the stain was compared with unstained controls via flow cytometry (BD FACScalibur). SYTOX Green was diluted from the supplied 5 mmol L<sup>-1</sup> in dimethylsulfoxide stock solution to 0.1 mmol L<sup>-1</sup> in Milli-Q water and stored frozen (–20°C) prior to use. CMFDA (Invitrogen C2925) was added to a final concentration of 10 μmol L<sup>-1</sup> and incubated for 60 min at culture temperature and light conditions. CMFDA was diluted to a concentration of 1 mmol L<sup>-1</sup> in acetone prior to use (Peperzak and Brussaard 2011) before aliquoting and storage at –20°C. SYTOX Green and CMFDA final

concentration and incubation time were optimized prior to use using heat-killed cells (80°C, 5 min) and the “maximum fluorescence ratio” approach (Brussaard et al. 2001). We used an adaptation of the protocol of Bidle and Bender (2008) to detect caspase-like activity: cells were stained *in vivo* with a fluorescein isothiocyanate conjugate of carbobenzoxy-valyl-alanyl-aspartyl-[O-methyl]-fluoromethylketone to label cells containing activated caspases (CaspACE; Promega G7462). Caspases are proteases thought to be specific to PCD (*see* Discussion). CaspACE was added to cells at a final concentration of 0.5  $\mu\text{mol L}^{-1}$  and incubated for 30 min at culture temperature in the dark, before flow cytometric analysis. For all stains working stocks were kept at  $-20^\circ\text{C}$  before use. We used Milli-Q water as a sheath fluid, analyses were triggered on red fluorescence, using “lo” flow ( $\sim 20 \mu\text{L min}^{-1}$ ), and 10,000 events were collected. We used an event rate between 100 and 400 cells  $\text{s}^{-1}$  to avoid coincidence and when needed, samples were diluted in 0.1- $\mu\text{m}$ -filtered artificial seawater prior to analysis. Flowset beads (Beckman-Coulter) were analyzed at the beginning of each set of measurements, and bead fluorescence was used to normalize stain fluorescence (Marie et al. 2005).

**Photosynthetic pigments**—Culture samples (20–25 mL) were centrifuged ( $5300 \times g$ , 20 min,  $8^\circ\text{C}$ ), the supernatant discarded and cells were flash frozen in liquid  $\text{N}_2$  and stored at  $-80^\circ\text{C}$  until analysis. Samples were extracted in 0.5 mL of acetone under dim light by sonication (amplitude 35%, Vibra Cell Probe; Sonics) for 45 s. The extract was clarified by centrifugation ( $10,956 \times g$ , Microcentrifuge 5415; Eppendorf). Reversed-phase HPLC was conducted using an Agilent 1200 system with photodiode array detector. Instrument control, data processing, and analysis were performed using Chemstation software. Separations were performed in the reversed-phase mode using two Waters Spherisorb ODS2 C18 3- $\mu\text{m}$  columns ( $150 \times 4.6$  mm internal diameter [i.d.]) in-line with a pre-column containing the same phase ( $10 \times 5$  mm i.d.). A Phenomenex pre-column filter (Security Guard, ODS C18,  $4 \times 3$  mm i.d.) was used to prevent rapid deterioration of the pre-column. Elution was carried out using a mobile phase gradient comprising acetonitrile, methanol, 0.01 mol  $\text{L}^{-1}$  ammonium acetate, and ethyl acetate at a flow rate of 0.7 mL  $\text{min}^{-1}$  (Method C in Airs et al. 2001). All solvents were HPLC grade. LC-MS analysis was performed using an Agilent 1200 HPLC with photodiode array detection coupled via an atmospheric pressure chemical ionization (APCI) source to an Agilent 6330 ion trap mass spectrometer. The HPLC conditions used were as described above. The mass spectrometer was operated in the positive ion mode. LC-MS settings were as follows: drying temperature  $350^\circ\text{C}$ , APCI vaporizer temperature  $450^\circ\text{C}$ , nebulizer 414 kPa, drying gas 5 L  $\text{min}^{-1}$ , capillary voltage  $-4500$  V. Methanoic acid was added to the HPLC eluent post-column at a flow rate of 5  $\mu\text{L min}^{-1}$  to aid ionization (Airs and Keely 2000). Using a combination of high-resolution HPLC and LC-MS (Airs et al. 2001) enabled separation and structural assignment of chlorophyll alteration products present in the samples, as well as routinely detected chlorophylls and carotenoids.

**DMSP and DMS**—Five milliliters of culture was sampled using gastight syringes and gently filtered (25-mm Whatman GF/F) using a Swinnex unit. The filter was then placed into a 4-mL vial containing 3 mL of 0.5 mol NaOH and immediately closed with a screw cap containing a polytetrafluoroethylene (PTFE)-silicone septum (Alltech). The vials were kept in the dark and placed in a constant-temperature heating block at  $30^\circ\text{C}$  overnight to equilibrate. The headspace of the vial was then analyzed for DMS by piercing the septum with a gastight syringe and injecting 50  $\mu\text{L}$  into a gas chromatograph (Shimadzu GC-2010 with flame photometric detection). The amount of DMSP particulate on the filter was then calculated with reference to standard curves and expressed as a concentration in the cells (Steinke et al. 2000). The filtrate was purged immediately to analyze culture DMS concentration. The filtrate was purged for 15 min ( $\text{N}_2$ , 60 mL  $\text{min}^{-1}$ ) in a cryogenic purge-and-trap system; DMS was trapped in a Teflon loop ( $-150^\circ\text{C}$ ), flash evaporated by immersing the loop in boiling water, and then injected into the gas chromatograph (Turner et al. 1990). After purging the DMS from the filtrate, the concentration of DMSP<sub>dissolved</sub> was determined by transferring 4 mL of the purged filtrate into a 20-mL crimp vial, to which 1 mL of 10 mol NaOH was added and topped up with 10 mL of distilled water to maintain a constant analytical volume of 15 mL. The vial was immediately closed with a Teflon-coated septum and later analyzed by the headspace technique. DMSP<sub>total</sub> was measured in an unfiltered volume of culture hydrolyzed with 0.5 mL of 10 mol NaOH in a vial sealed gastight with a PTFE-silicone septum.

## Results

**Cell culture and growth measurements**—To minimize the presence of dead cells and debris in the cultures at the beginning of the experiment, cultures were closely monitored and grown in semi-continuous mode before measurements commenced. From preliminary work it was clear that both *E. huxleyi* and *T. pseudonana* biomass would consistently achieve a final yield of  $\sim 2.5 \times 10^6$  cells  $\text{mL}^{-1}$  with a specific growth rate ( $\mu \text{d}^{-1}$ ) of 0.6 under our culture conditions. By calculation, nitrogen should have been limiting in both species at this point assuming cells were using nutrients in the Redfield ratio. We performed “add-back” experiments to test what controlled limitation (data not shown). These experiments indicated that for *T. pseudonana* nitrogen clearly caused growth limitation; when nitrate was added back, cell number increased. The pattern for *E. huxleyi* was less clear, as no obvious increase in *E. huxleyi* biomass was stimulated by adding back either nitrate or phosphate. After the onset of stationary phase, *E. huxleyi* cell number remained constant for 20 d, whereas *T. pseudonana* cell number began to decline after 5 d, and over the next 20 d declined by 65% (Fig. 1A). *E. huxleyi* coccosphere volume increased after the growth phase from a mean of about 35  $\mu\text{m}^3$  to almost 80  $\mu\text{m}^3$  at the end of the stationary phase. *T. pseudonana* also increased in cell volume, but by less than *E. huxleyi* coccosphere volume; the increase in cell volume stabilized after the growth phase

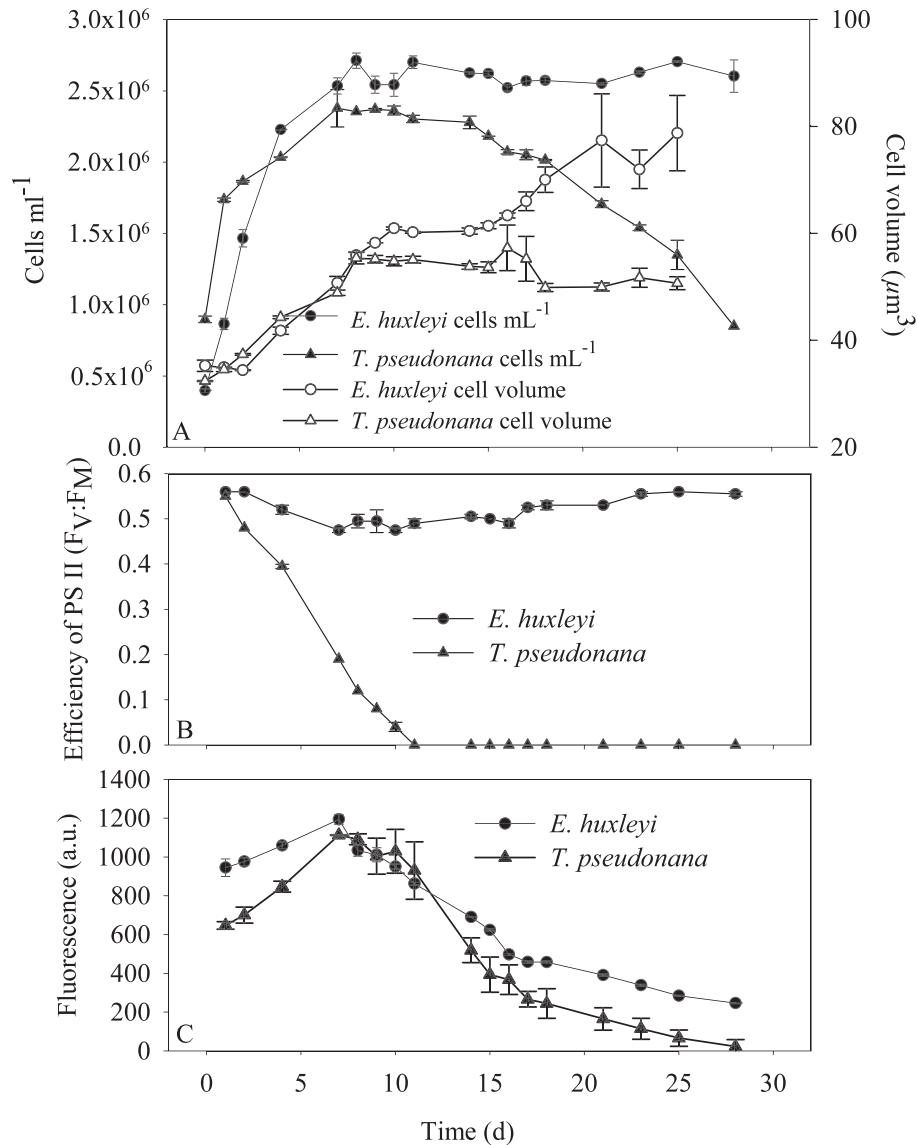


Fig. 1. (A) Cell number and cell volume, (B) efficiency of Photosystem II (dark-adapted  $F_v:F_M$ ), and (C) in vivo fluorescence in duplicate *Emiliania huxleyi* and *Thalassiosira pseudonana* batch cultures (mean and standard error) during cell division, the transition from cell division to stationary phase, and the death phase (*T. pseudonana* only).

at about  $50 \mu\text{m}^3$  (Fig. 1A). *T. pseudonana* dark-acclimated  $F_v:F_M$  (maximum Photosystem II efficiency [PS II efficiency]; Kromkamp and Forster 2003) declined from a maximum of 0.6 in early log-phase to zero after 5 d in stationary phase. *E. huxleyi* dark-acclimated  $F_v:F_M$  remained constant at  $\sim 0.5$  (Fig. 1B). Culture fluorescence declined after the onset of stationary phase in both species (Fig. 1C). During this decline it was possible to discriminate two subpopulations by flow cytometry (see below).

**Flow cytometry and cell staining**—Light scattering: Over the transition from growth to stationary phase *E. huxleyi* forward scatter increased and side scatter became more variable. An increase in *T. pseudonana* forward scatter was

also evident over the transition, but no obvious change in side scatter developed (data not shown).

**Pigment fluorescence:** During growth all *E. huxleyi* cells had the same, slightly increasing, pigment fluorescence (data not shown). During the stationary phase all cells declined in pigment fluorescence and a “low-red” subpopulation developed (Fig. 2). This subpopulation doubled in size during the stationary phase, from  $\sim 6\%$  to  $12\%$  of all cells. Low-red *E. huxleyi* cells were not obviously different in terms of forward and side scatter compared to “normal” cells. *T. pseudonana* cells also declined in average pigment fluorescence after the onset of stationary phase and low-red cells accounted for almost 50% of cells toward the end of the sampling period. As in *E. huxleyi*, *T. pseudonana* low-red cells did not obviously

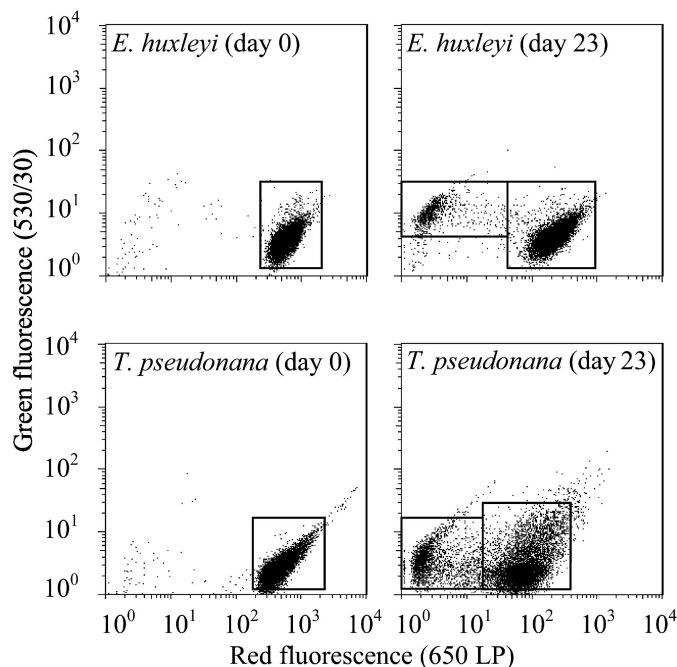


Fig. 2. Representative biparametric plots of red and green fluorescence in *Emiliania huxleyi* and *Thalassiosira pseudonana* batch cultures. The plots indicate the process of chlorosis (the reduction in cellular pigment fluorescence over time) in batch cultures. At day 0 both species show single populations with consistently high-red (pigment) fluorescence; by day 23 two populations are apparent and are highlighted by the regions overlaid on the plot. Cells transitional between the two states are visible, indicating that the low-red population arises via chlorosis of the high-red population.

differ from normal cells in their forward and side scatter characteristics (data not shown).

**SYTOX Green staining:** *E. huxleyi* showed < 5% labeled cells throughout the experiment; neither the low-red nor normal cells labeled with SYTOX Green, indicating that almost all cells, of both cell types, had intact plasma membranes over the duration of the monitoring period. In contrast, *T. pseudonana* had low numbers of labeled cells (< 2%) until the stationary phase, whereupon the percentage of labeled cells rose rapidly to a maximum of 25% on the last sampling day (Fig. 3).

**CMFDA staining:** Within the growth phase *E. huxleyi* cells showed clear differences in CMFDA metabolism. Most cells metabolized the probe and become highly fluorescent; however, about 20% of cells showed no increased fluorescence and were similar to unstained controls (Fig. 4A). This difference remained roughly constant throughout the stationary phase (Fig. 4B). Further, in *E. huxleyi* the “high CMF” population increased their CMFDA metabolism in the stationary phase (Fig. 4C). The low-red *E. huxleyi* cells that increased slightly in abundance throughout the experiment did not metabolize the probe; low-red cell green fluorescence was comparable to unstained cells. *T. pseudonana* did not show this intrapopulation variability; all cells within the population exhibited a significant decline (linear regression;  $p =$

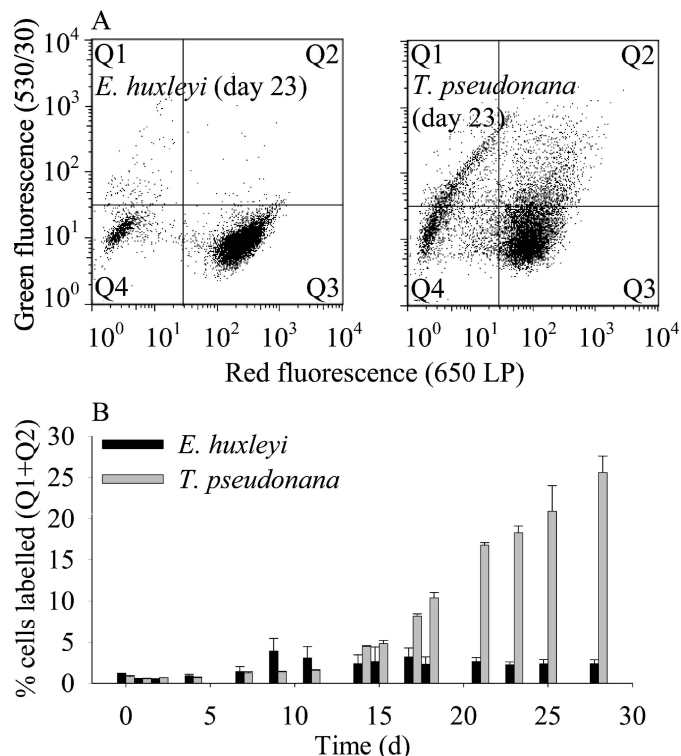


Fig. 3. Membrane permeability (SYTOX Green staining) during nutrient depletion in *Emiliania huxleyi* and *Thalassiosira pseudonana*. (A) shows representative biparametric plots for both species at day 23. (B) shows the % of SYTOX-stained cells over time (mean and standard error). Note that “stained cells” = Q1 + Q2. Q1 = stained debris and stained “low-red” cells, Q2 = stained “normal” cells, Q3 = unstained normal cells, and Q4 = unstained debris and unstained low-red cells.

0.001) in CMFDA fluorescence over the transition from active growth to stationary phase (Fig. 4C). However, even in the death phase, *T. pseudonana* cells showed CMFDA fluorescence that was elevated relative to unstained controls (data not shown).

**CaspACE staining:** *E. huxleyi* CaspACE fluorescence increased during the experiment with both types of cells (normal and low red), showing a similar level of fluorescence due to CaspACE binding. Among normal *E. huxleyi* cells there was a significant increase (linear regression;  $p = 0.001$ ) in CaspACE binding over time (Fig. 5). There was no significant trend (linear regression;  $p = 0.05$ ; Fig. 5) in *T. pseudonana* CaspACE fluorescence with time, and as with *E. huxleyi* cells, there was no obvious difference between normal and low-red *T. pseudonana* cells (data not shown).

**Photosynthetic pigments—Chemical assignment:** During reversed-phase HPLC, chlorophyll allomers typically elute in the region of the chromatogram immediately prior to Chl *a* (Walker et al. 2002) and most exhibit ultraviolet-visible spectra indistinguishable from Chl *a*. In extracts from this study, five components (I–V; Fig. 6) eluted in the region expected for chlorophyll allomers. Components I

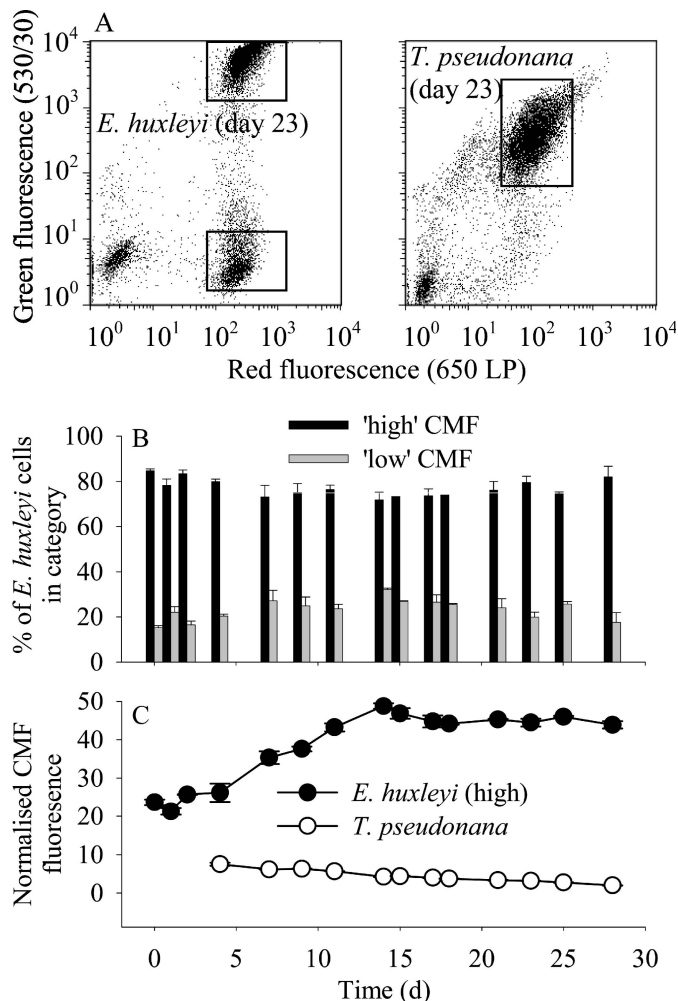


Fig. 4. Hydrolytic enzyme activity (CMFDA staining) during nutrient depletion in *Emiliana huxleyi* and *Thalassiosira pseudonana*. (A) shows representative biparametric plots for both species at day 23: note the clear separation of the *E. huxleyi* population into a “high” and “low” CMF population as indicated by the superimposed regions on the plot. (B) shows relative % of high- and low-CMF cells over the course of growth and stationary phase in *E. huxleyi*. Finally, (C) shows normalized CMF fluorescence within the high *E. huxleyi* population and all *T. pseudonana* cells (mean and standard error). Note: CMF fluorescence was normalized to a fluorescence standard, flowset beads (see text), which were analyzed simultaneously.

and III were assigned as  $^{132}$ -hydroxy-chlorophyll *a* (see structure inset, Fig. 6) and  $^{132}$ -hydroxy-chlorophyll *a'*, and components IV and V were assigned as (*S*)- $^{132}$ -methoxy-chlorophyll *a* and (*R*)- $^{132}$ -methoxy-chlorophyll *a*, respectively, by comparison to published MS/MS data (Table 1; Walker et al. 2002). Component II exhibited similar analytical data to Chl *a* (Table 1), showing a 2-Da difference in protonated molecule and common major ions in MS<sup>2</sup> (Table 1). The phytol chain of Chl *a* is lost as phytadiene, resulting in a loss of 278 Da during APCI-LC-MS<sup>n</sup> (Airs et al. 2001; Table 1). The loss of 276 Da from the protonated molecule of Component II indicates that the structural difference from Chl *a* originates on the phytol chain and is likely to be due to an additional double bond.

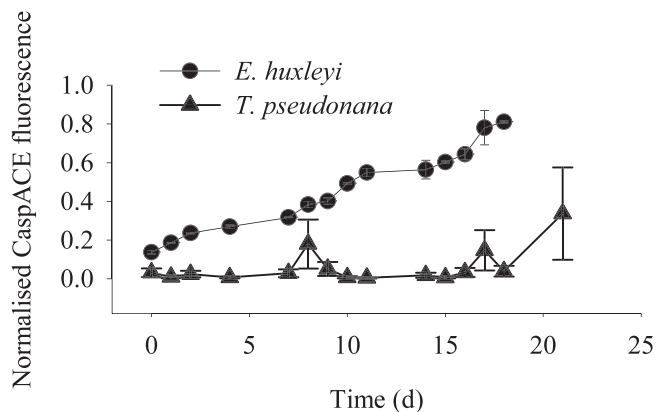


Fig. 5. Changes in CaspACE binding in normal cells (see text) during nutrient depletion in *Emiliana huxleyi* and *Thalassiosira pseudonana* batch cultures (mean and standard error). Note: CaspACE fluorescence was normalized to a fluorescence standard, flowset beads (see text), which were analyzed simultaneously.

This component has been assigned previously in a culture of *Pavlova gyrams* (Bale 2010). One of the final stages in the biosynthesis of Chl *a* is the conversion of geranylgeraniol to phytol by saturation of three of its double bonds (Rudiger 2006). Component II, referred to hereafter as Chl *a*<sub>P276</sub>, may therefore be a biosynthetic precursor to Chl *a*.

**Pigment changes during growth limitation**—Of the alteration products observed, methoxychlorophyll *a* was present at highest concentrations relative to Chl *a* in both *E. huxleyi* and *T. pseudonana* (Fig. 7A). In both cultures Chl *a*<sub>P276</sub> was highest in the active growth phase, consistent with its assignment as a biosynthetic precursor to Chl *a*. In *T. pseudonana*, methoxychlorophyll *a* increased relative to Chl *a* during the transition from cell division to the stationary phase (Fig. 7A). The concentration of methoxychlorophyll *a* stayed high relative to Chl *a* into the diatom death phase, before declining to undetectable levels (Fig. 7A). The ratio of hydroxychlorophyll *a*: Chl *a* showed a slight increase in *T. pseudonana* during the transition, mirroring the profile of methoxychlorophyll *a*. No increase in the ratio of methoxychlorophyll or hydroxychlorophyll *a* to Chl *a* was observed in *E. huxleyi* cultures (Fig. 7A). The carotenoid: Chl *a* ratio remained constant in *E. huxleyi* (Fig. 7B) but steadily increased in *T. pseudonana*. In *E. huxleyi*, the reduction in carotenoids closely tracked the reduction in chlorophyll, consistent with a controlled reduction of cellular pigment concentration. In *T. pseudonana*, the increase in the carotenoid: chlorophyll ratio occurred because of a more rapid decrease in chlorophyll relative to carotenoids.

**DMSP and DMS**—Over the course of the experiment, *E. huxleyi* cultures significantly (linear regression;  $p = 0.001$ ) accumulated DMSP (DMSP<sub>total</sub>), whereas *T. pseudonana* DMSP<sub>total</sub> showed no significant relationship with time ( $p = 0.05$ ). Within the *T. pseudonana* data set, however, a decline in DMSP<sub>total</sub> is suggested within the stationary/death phase (Fig. 8A). The intracellular concentration of DMSP (DMSP<sub>cell</sub>; Fig. 8B) showed no significant trend with time ( $p = 0.05$ ) in both species over the whole course

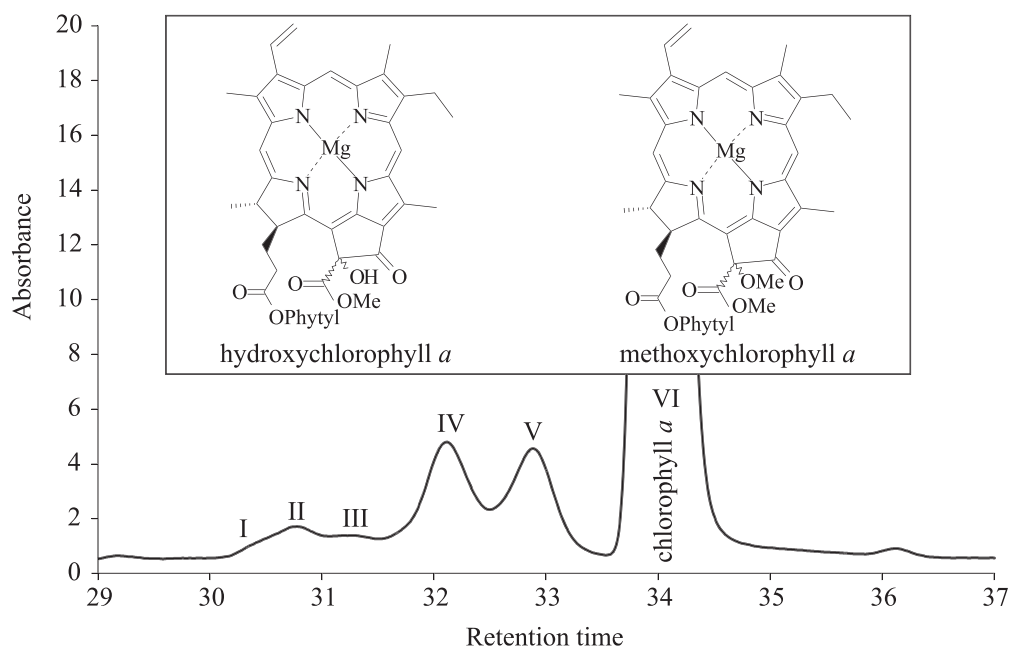


Fig. 6. Partial HPLC chromatogram (660 nm) showing elution position (relative to Chl *a*) of chlorophyll alteration products detected. For peak assignments see Table 1.

of the experiment, and was consistent within the stationary/death phase at  $\sim 120 \text{ mmol L}^{-1}$  (*E. huxleyi*) and  $35 \text{ mmol L}^{-1}$  (*T. pseudonana*). However, between days 0 and 10 there was a notable increase in *T. pseudonana*  $\text{DMSP}_{\text{cell}}$  from  $0.7$  to  $34 \text{ mmol L}^{-1}$ . The divergence between  $\text{DMSP}_{\text{total}}$  and  $\text{DMSP}_{\text{cell}}$  in *E. huxleyi* can be explained by the increased coccosphere volume in stationary phase; *E. huxleyi* coccosphere volume increased with time (Fig. 1A). The concentration of DMS in both cultures increased significantly over the course of the experiment ( $p = 0.05$ ). In *T. pseudonana* DMS increased from  $5 \text{ nmol L}^{-1}$  to  $90 \text{ nmol L}^{-1}$  and from  $10 \text{ nmol L}^{-1}$  to  $42 \text{ nmol L}^{-1}$  in *E. huxleyi* (Fig. 8C).  $\text{DMSP}_{\text{dissolved}}$  increased in both species after the growth phase, to around  $2 \text{ } \mu\text{mol L}^{-1}$  in *E. huxleyi* and around  $1.25 \text{ } \mu\text{mol L}^{-1}$  in *T. pseudonana* (data not shown).

## Discussion

The main finding of our work was that the response of the two model species to nutrient limitation was quite different. Establishing the specific nutrient that is limiting is important to place the work into an environmental context. Add-back experiments are a useful way of verifying the limiting nutrient (La Roche et al. 1993) and clearly indicated nitrogen limitation as the cause of growth limitation in our *T. pseudonana* cultures. The add-back data were ambiguous for *E. huxleyi*. We suggest that the timing of the add-back is important and we may have been too late in adding the nutrients (which we did just before the plateau). We hypothesize that *E. huxleyi* cells may have already committed to transforming into a “persister” form by the time the extra nutrients were delivered and thus the add-back of limiting nutrient had no effect. We find the fact that Loebel et al. (2010) find similar patterns in *E.*

*huxleyi* PS II efficiency, and biomass, under nitrogen deprivation quite compelling as it provides support for nitrogen being the cause of growth limitation in our experiments. However, Loebel et al. (2010) used a different type of experimental manipulation (centrifugation of cells and resuspension in nitrogen-free media), which would have resulted in somewhat different environmental conditions for the cells. Regardless of the method of inducing nitrogen limitation, however, the tolerance of *E. huxleyi* to endure growth-limiting conditions was clearly superior to that of *T. pseudonana*.

Knowing whether cells are viable is important in order to scale metabolic parameters such as exudation rates or primary production (Garvey et al. 2007). In this study, we have linked an assessment of viability with the alteration of two classes of compounds important in biogeochemical cycles. Viability is “the quality or state of being viable; the capacity for living; the ability to live under certain conditions” (*Oxford English Dictionary*), and in cell biology, the concept of viability is generally extended to a notion of having the capacity to divide in the future. Whether or not a cell divides in the future will be determined by the environment, and the environment may change. Therefore, it is difficult to assess viability with existing live/dead staining techniques, as these do not reveal the capacity for cell division after being stained. Indeed, some staining procedures can themselves be toxic (e.g., some DNA stains; Nebe-von-Caron 2000), precluding a sort of cells on the basis of their staining characteristics and subsequent monitoring for cell division. Instead, live and dead staining methods test some physiological correlate of being alive, such as membrane permeability or enzyme activity. Such physiological correlates are “validated” by abolishing them via cell killing with heat, chemical fixation, or some other method. Since it is possible

Table 1. Assignment of chlorophyll and related alteration products in cultures of *Emiliania huxleyi* and *Thalassiosira pseudonana*. UV-vis, ultraviolet–visible.

Peak No.	Main UV-vis absorption bands (nm)	Full MS and MS <sup>2</sup> ions*†	Assignment
I	430, 664	Full MS: [M+H] <sup>+</sup> 887 (100); MS <sup>2</sup> (887): 869 ([M+H] <sup>+</sup> -18; 2), 609 ([M+H] <sup>+</sup> -278; 100), 591 ([M+H] <sup>+</sup> -278-18; 50), 549 ([M+H] <sup>+</sup> -278-60; 15)	Hydroxychlorophyll <i>a</i>
II	432, 664	Full MS: [M+H] <sup>+</sup> 869 (100); MS <sup>2</sup> (869): 837 ([M+H] <sup>+</sup> -32; 5), 593 ([M+H] <sup>+</sup> -276; 100), 533 ([M+H] <sup>+</sup> -276-60; 80)	Chlorophyll <i>a</i> <sub>p276</sub>
III	432, 664	Full MS: [M+H] <sup>+</sup> 887 (100); MS <sup>2</sup> (887): 869 ([M+H] <sup>+</sup> -18; 5), 609 ([M+H] <sup>+</sup> -278; 100), 591 ([M+H] <sup>+</sup> -278-18; 50), 549 ([M+H] <sup>+</sup> -278-60; 10)	Hydroxychlorophyll <i>a</i> '
IV	422, 664	Full MS: [M+H] <sup>+</sup> 901 (60), 869 (100); MS <sup>2</sup> (901): 869 ([M+H] <sup>+</sup> -32; 25), 623 ([M+H] <sup>+</sup> -278; 10), 591 ([M+H] <sup>+</sup> -278-32; 100), 559 ([M+H] <sup>+</sup> -278-32-32; 15), 531 ([M+H] <sup>+</sup> -278-32-60; 40); MS <sup>2</sup> (869): 591 ([M+H] <sup>+</sup> -278; 100), 559 ([M+H] <sup>+</sup> -278-32; 15), 531 ([M+H] <sup>+</sup> -278-60; 30)	Methoxychlorophyll <i>a</i>
V	420, 662	Full MS: [M+H] <sup>+</sup> 901 (90), 869 (100); MS <sup>2</sup> (901): 869 ([M+H] <sup>+</sup> -32; 2), 623 ([M+H] <sup>+</sup> -278; 60), 591 ([M+H] <sup>+</sup> -278-32; 60), 559 ([M+H] <sup>+</sup> -278-32-32; 5), 531 ([M+H] <sup>+</sup> -278-32-60; 50); MS <sup>2</sup> (869): 591 ([M+H] <sup>+</sup> -278; 100), 559 ([M+H] <sup>+</sup> -278-32; 5), 531 ([M+H] <sup>+</sup> -278-60; 30)	Methoxychlorophyll <i>a</i> '
VI	432, 664	Full MS: [M+H] <sup>+</sup> 871 (100); MS <sup>2</sup> (871): 839 ([M+H] <sup>+</sup> -32; 5), 593 ([M+H] <sup>+</sup> -278; 100), 533 ([M+H] <sup>+</sup> -278-60; 75)	Chl <i>a</i>

\* All chlorophyll derivatives appear as demetallated ions due to post-column demetallation prior to sequential mass scanning (Airs and Keely 2000; *see* Methods).  
 † Full MS: relative abundance shown in parentheses. MS<sup>2</sup>: precursor ion indicated in parentheses. MS<sup>2</sup> ions: relationship to [M+H]<sup>+</sup> and relative abundance indicated in parentheses.

to generate a complicated spectrum of states with such methods, making simple categorization difficult, and the performance of the stains is variable between species (Brussaard et al. 2001), the use of live/dead stains has been limited in eukaryotic microbial ecology (Garvey et al. 2007). Nevertheless, these methods are at present the “state of the art” and they have given valuable insight into the role of mortality in the microbial food web (Veldhuis et al. 2001). We show here that the coccolithophore *E. huxleyi* has a very different response to growth limitation from that of the diatom *T. pseudonana*. Benthic “resting stages” are known in a number of *Thalassiosira* species (Lewis et al. 1999), but during the decline in our cultures we saw no obvious change in cell morphology. The ability to form resting stages has not been recorded in this strain or clonal isolate, and even if this ability did exist, it may have been lost in culture. *T. pseudonana* biomass remained constant for ~ 8 d before cell loss due to lysis became apparent (Fig. 1A) and throughout this period the PS II efficiency declined in a pattern similar to that seen in *T. weissflogii* (Berges and Falkowski 1998), likely indicating a process of intracellular protein degradation brought about by nitrogen deprivation. Such internal degradation leads to a dismantling of the photosynthetic apparatus and the loss of photosynthetic pigment fluorescence. Both of these processes were very clear in our data set; the loss of pigment fluorescence (“chlorosis”; Geider et al. 1993) correlated with decreased enzyme activity and increased membrane permeability. This process was especially clear in the diatom but a more subtle process occurred in the coccolithophore. Fluorescence due to CaspACE binding did not increase during the decline in diatom biomass.

Using the same strain of *T. pseudonana* (CCMP 1335), Bidle and Bender (2008) noted increased CaspACE binding (expressed as % of cells stained) during the cell lysis of *T. pseudonana* after stationary phase. Even higher binding was observed in Fe-limited biomass declines, and CaspACE binding was most prominent in cells with low fluorescence. Upregulation of caspases may therefore be more likely under Fe-limited conditions. An ongoing difficulty in the use of caspase-activity stains in the interpretation of cell death processes is the lack of good positive controls. Cell differentiation to a resting stage is not a recognized pathway in coccolithophores, which may instead switch to a motile, haploid form during stressful conditions and thereby exploit a different ecological niche (Frada et al. 2008). However, the persistence of *E. huxleyi* during stationary phase in our study did not seem to be accompanied by meiosis, as assessed by periodic microscopy on our cultures. Increases in intracellular enzyme activity were clear from both CMFDA and CaspACE results, highlighting perhaps the requirement for hydrolytic enzymatic activity to be present in the cell for the successful detection of caspase-like activity. In the absence of other measurements (*see* below), there are three interpretations of increased CaspACE binding in *E. huxleyi*: (1) an increase in proteolytic activity within the cell related to a shift to a low metabolic state (which nevertheless retains photosynthetic pigmentation); or (2) intracellular reorganization related to the induction of meiosis; or (3) PCD in moribund cells, potentially leading to an apoptotic morphology but with intact plasma membranes (the timing of membrane permeability failure may therefore be late in *E. huxleyi* PCD). Of these two possibilities we suggest that (1) or (2) is

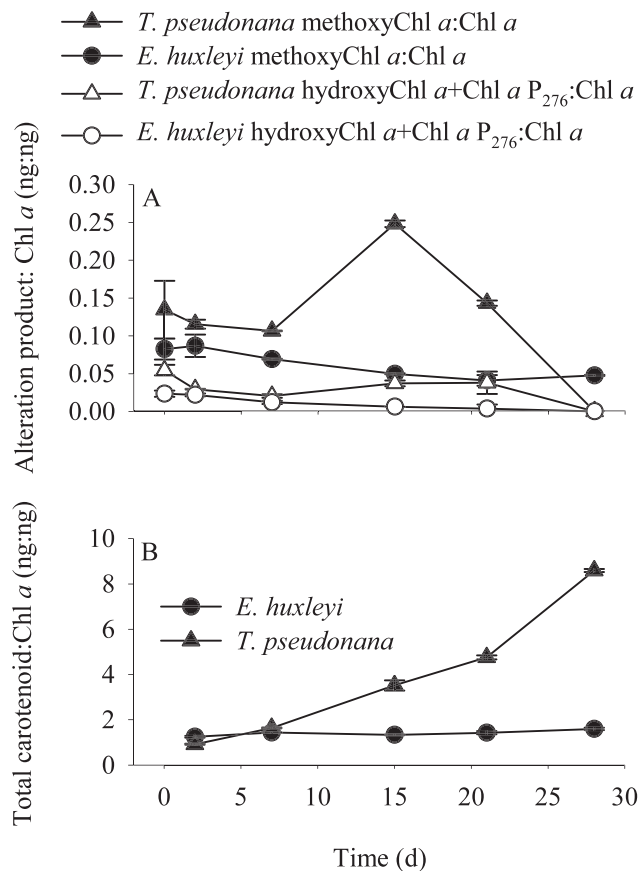


Fig. 7. (A) Ratio of total methoxychlorophyll *a* to Chl *a* and total hydroxychlorophyll *a* + Chl *a*<sub>P276</sub> to Chl *a* in *Thalassiosira pseudonana* and *Emiliania huxleyi* and (B) ratio of total carotenoid to Chl *a* in *T. pseudonana* and *E. huxleyi* (mean and standard error) in nutrient-limited batch cultures.

the safest interpretation because we do not have accompanying measurements of the other processes thought to be part of PCD and which would result in apoptosis (e.g., DNA fragmentation, phosphatidylserine inversion). Additional complications in the interpretation of the CasPACE data are that caspases may have alternative functions to PCD (Lamkanfi et al. 2007); in general, the clan to which caspases belong (clan CD, family C14) is poorly understood in protists (Vercammen et al. 2007).

Although our two species showed different responses to growth limitation in many respects, one common element was the formation of low-red or chlorotic cells. As a proportion of the total cell population, chlorotic cells became more abundant in the diatom cultures. The formation of chlorotic cells has been well noted before, in diatoms (*Phaeodactylum tricorutum*; Geider et al. 1993) and also in cyanobacteria (*Synechococcus* PCC 7942; Sauer et al. 2001). After the onset of nitrogen deprivation, *Synechococcus* PCC 7942 shows an immediate and substantial reduction in protein content, leading to the formation of an ultra-low metabolism resting stage (Sauer et al. 2001). In *P. tricorutum* cell pigmentation changes rapidly as part of an adaptive and reversible response to self-shading, thereby tuning photosynthetic activity to the

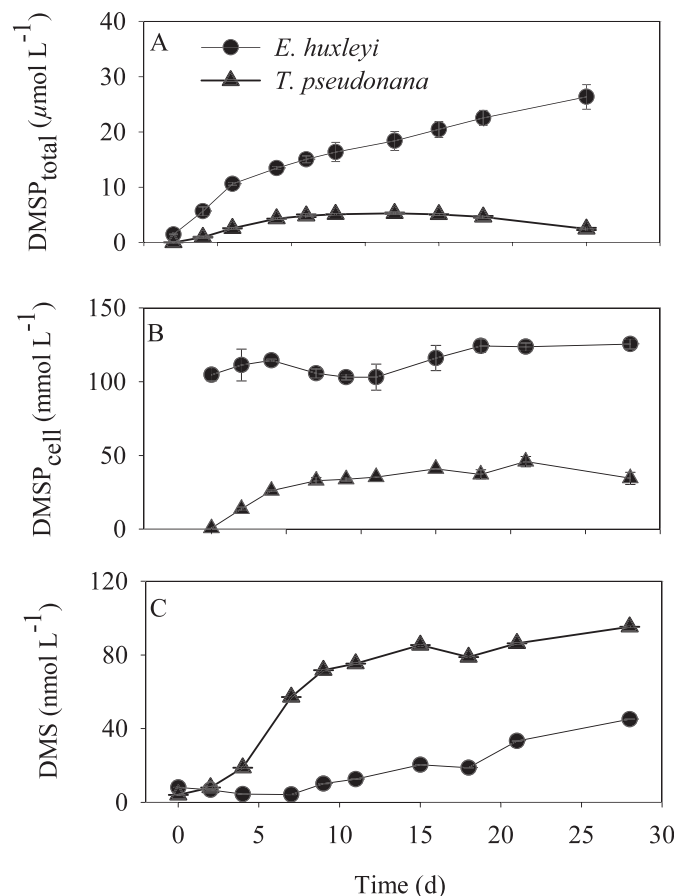


Fig. 8. (A) DMSP<sub>total</sub> (μmol L<sup>-1</sup>), (B) DMSP<sub>cell</sub> (mmol L<sup>-1</sup>), and (C) DMS (nmol L<sup>-1</sup>) in duplicate *Emiliania huxleyi* (circles) and *Thalassiosira pseudonana* (triangles) batch cultures (mean and standard error) over the batch growth cycle.

available resources. Given our data set, it appears the response of *E. huxleyi* to nutrient limitation resembles that of *Synechococcus* in that while there was an immediate change in pigment content per cell, photosynthetic efficiency was unchanged and there was also no change in the pigment profile. Such a conclusion is reinforced by the recent finding that the high PS II repair capability of *E. huxleyi* means that it is well adapted to endure nutrient deplete conditions (Loebl et al. 2010). In contrast, *T. pseudonana* showed a rapid decline in photosynthetic efficiency as pigment content declined and the pigment profile also changed. It is possible that the formation of chlorotic cells had different causes: in *E. huxleyi*, where the proportion of chlorotic cells did not increase as much as in the diatom population, the ultimate cause of cell chlorosis may have been cell cycle stage at a critical point in the onset of nutrient deprivation, whereas in *T. pseudonana* the higher proportion of chlorotic cells after nutrient deprivation suggests that all cells were destined to share the same fate. These two ideas are not mutually exclusive, however, since we did not assess the degree of cell cycle synchrony; it may have been that the *T. pseudonana* cells were in synchronized division at the onset of nutrient deprivation. This seems unlikely; diatom cultures often require an

experimental treatment (such as silica starvation) to induce synchrony (Hildebrand et al. 2007) and were therefore unlikely to be undergoing synchronous division. Resolving population cell cycle stage in parallel with assessments of physiological staining would be beneficial in further investigations of these responses. In conclusion, CMFDA and SYTOX Green worked well as indicators of changing cell condition and yielded robust information. Our data set highlights the necessity of making observations over a relatively long period in order to gather context and to avoid simple categorizations (live or dead) without such context. The increase in *E. huxleyi* CMFDA fluorescence during the stationary phase, for example, clearly represents a process of cellular reorganization, but cells did not become “more alive.” Simplifications about cell states (e.g., “active” and “inactive”) remain difficult using existing methods. Bacterioplankton, for example, display an enormous range of metabolic states in natural populations (Smith and del Giorgio 2003; Pirker et al. 2005). Development of simultaneous and multi-staining approaches in eukaryotic microbiology should help in revealing all, or most, of the physiological heterogeneity within these populations.

This is the first study to investigate the formation of chlorophyll oxidation (allomer) products in conjunction with measurements of photosynthetic efficiency and loss of cell viability in phytoplankton cultures. The chlorophyll oxidation products detected, methoxychlorophyll and hydroxychlorophyll, are common products in laboratory studies of chlorophyll allomerization reactions (Hynninen and Hyvärinen 2002; Jie et al. 2002). Methoxychlorophyll *a*, however, has not been reported previously in eukaryotic phytoplankton. Methoxychlorophyll *a* and hydroxychlorophyll *a* increased relative to Chl *a* from day 30 onwards in *T. pseudonana* cultures, by which point the dark-acclimated  $F_V:F_M$  had declined from 0.6 to 0.1. In contrast to *T. pseudonana*, the relative concentration of hydroxychlorophyll *a* and methoxychlorophyll *a* remained constant in *E. huxleyi*, as did the dark-acclimated  $F_V:F_M$  and percentage of SYTOX Green-stained cells. Similarly, Bale (2010) found that the relative proportion of hydroxychlorophyll *a* remained constant in *E. huxleyi* over a 40-d period in batch culture. In *T. pseudonana*, the reduction in maximum PS II efficiency and increase in the relative abundance of chlorophyll oxidation products preceded the increase in the percentage of cells labeled with SYTOX Green. The relative increase in chlorophyll alteration products may therefore serve as an early indicator of loss of cell viability. Although methoxychlorophylls have not been reported previously in pigment studies of senescent phytoplankton, detritus, or sediments, they have been detected in cyanobacteria (R. A. Airs unpubl. data) and further high-resolution LC-MS studies may reveal methoxychlorophyll to be a common early-transformation product in phytoplankton. Hydroxychlorophyll *a* has been detected in field samples from phytoplankton blooms in the Celtic Sea and North Atlantic (Walker and Keely 2004; Bale 2010), and chlorophyll allomer-type components are commonly detected in field samples, even when routine rather than high-resolution HPLC methods are applied (R. A. Airs unpubl. data). From the higher relative abundance of

methoxychlorophyll *a* than hydroxychlorophyll *a* in our cultures, the detection of hydroxychlorophyll *a* in field samples indicates that the likelihood of detecting methoxychlorophyll *a* in field samples is good. The effect of these early chlorophyll alterations on the overall light absorption of the cell, and hence the potential of these alterations to be detected by remote methods is, however, unknown. A trace of pheophytin *a* (magnesium-free Chl *a*) was detected in both cultures throughout the experiment (data not shown), contributing at levels < 10% of the other chlorophyll alteration products detected. Pheophytin *a* has been shown to be present in healthy cells, due to its role as a primary electron acceptor of PS II (Klimov 2003). Both chlorophyllide *a*, and its magnesium-free counterpart pheophorbide *a*, have been associated with senescence in earlier studies (Jeffrey and Hallegraeff 1987; Louda et al. 2002). These compounds were not detected, however, during this study. How senescence is defined within an experiment, the method of senescence induction, the timescale of experiments, as well as the presence or absence of cellular enzymes (e.g., chlorophyllase), are likely to influence the specific alterations of Chl *a*.

There are a number of sources and sinks of DMS and its precursor DMSP within the microbial food web. The intracellular concentration of DMSP in phytoplankton cells is the primary driver of ecosystem DMS emission, and certain microalgae synthesize DMSP in response to environmental factors such as light (Archer et al. 2010) and nitrogen depletion (Bucciarelli and Sunda 2003). DMSP can be released from algal cells by grazing and viral lysis, and these pathways may also elevate DMS levels by bringing algal enzymes that release DMS from DMSP into more intimate contact with the substrate (Stefels et al. 2007). In addition, bacteria demethylate DMSP, release DMS from DMSP, and oxidize DMS to dimethylsulfoxide (DMSO) (Schäfer et al. 2010). Depending upon the bacterial genera present and pathways involved, the DMS concentration can increase or decrease. However, it is interesting to note that the direct release by phytoplankton cells is suggested by modeling work to be the dominant factor in explaining natural DMS seasonality (Gabric et al. 2008).

In order to be useful as an antioxidant or an overflow compound, the intracellular concentration of DMSP would need to vary actively in response to environmental stress. To estimate intracellular DMSP concentration, it is necessary to have an accurate estimate of cell volume. In coccolithophores, this is complicated by the presence of the coccolith layer, the coccosphere, around the cell and in diatoms the intracellular vacuolar space provides a similar complication. During the stationary phase, coccolithophore calcification can continue after cell division stops (Lakeman et al. 2009), potentially leading to multilayered coccospheres. Acidification can remove coccoliths prior to cell volume measurement, but unfortunately we did not do this in the present study, so our conclusion of a constant  $DMSP_{cell}$  concentration in stationary-phase *E. huxleyi* is based on an assumption of increasing cell volume. Stefels et al. (2007) point out that cells generally decrease in volume with nitrogen starvation. It is possible that in the

present study the cell volume decreased while overall coccosphere volume increased, in which case intracellular DMSP concentration would also have increased. We recommend measuring acidified and non-acidified samples for volume estimates in future studies. The realization of how important this can be is currently spreading, with some studies (Archer et al. 2010) acidifying to make accurate estimates of cell volume whereas older studies tended not to do this. We are not aware of any studies quantifying vacuolar changes in *T. pseudonana* during nutrient limitation and, taking our data at face value, the 50-fold increase in intracellular DMSP concentration with nitrogen starvation confirms our original hypothesis. In nutrient-replete culture diatoms generally have lower concentrations of DMSP than representatives of other major phytoplankton groups (Stefels et al. 2007), so it has often been assumed that diatoms cannot be a major source of DMS in the marine environment. However, considering the data presented here and elsewhere (Sunda et al. 2002; Bucciarelli and Sunda 2003; Harada et al. 2009), alongside estimates that diatom primary production accounts for ~ 40% of the global total (Falkowski et al. 1998), it is clear that the overall diatom contribution may be greater than previously assumed.

Our study indicates that two important phytoplankton species have fundamentally different responses to nutrient deprivation. These different responses reflect the ecology of their groups in nature, and our assessment of physiological state reveals that *E. huxleyi* is much better able to cope with nutrient deprivation than *T. pseudonana*, through a cellular reorganization that may involve caspase-like activity and DMSP production. *T. pseudonana* shows a substantial increase in DMSP concentration in response to nitrogen limitation, and dies and lyses rapidly. We show for the first time that methoxychlorophyll *a* appears in *T. pseudonana* before membrane permeability is lost and lysis begins. Methoxychlorophyll *a* could therefore be a useful indicator of diatom senescence.

#### Acknowledgments

We thank the U.K. Natural Environment Research Council for funding this research (NE/E003974/1) and Rob Utting and Gareth Lee for technical help. We also thank the two anonymous reviewers who provided constructive comments. Additional support was provided by a British Council studentship to M.F. (UK India Education and Research Initiative).

#### References

- AGUSTÍ, S. 2004. Viability and niche segregation of *Prochlorococcus* and *Synechococcus* cells across the Central Atlantic Ocean. *Aquat. Microb. Ecol.* **36**: 53–59, doi:10.3354/ame036053
- AIRS, R. L., J. E. ATKINSON, AND B. J. KEELY. 2001. Development and application of a high resolution liquid chromatographic method for the analysis of complex pigment distributions. *J. Chromatogr. A* **917**: 167–177, doi:10.1016/S0021-9673(01)00663-X
- , AND B. J. KEELY. 2000. A novel approach for sensitivity enhancement in atmospheric pressure chemical ionization liquid chromatography/mass spectrometry. *Rapid Commun. Mass Spectrom.* **14**: 125–128, doi:10.1002/(SICI)1097-0231(2000215)14:3<125::AID-RCM847>3.0.CO;2-6
- ARCHER, S. D., M. RAGNI, R. WEBSTER, R. L. AIRS, AND R. J. GEIDER. 2010. Dimethyl sulfoniopropionate and dimethyl sulfide production in response to photoinhibition in *Emiliania huxleyi*. *Limnol. Oceanogr.* **55**: 1579–1589, doi:10.4319/lo.2010.55.4.1579
- BALE, N. 2010. Type I and Type II chlorophyll-*a* transformation products associated with phytoplankton fate processes. Ph.D. thesis. Univ. of Bristol.
- BEHRENFELD, M. J., AND E. BOSS. 2006. Beam attenuation and chlorophyll concentration as alternative optical indices of phytoplankton biomass. *J. Mar. Res.* **64**: 431–451, doi:10.1357/002224006778189563
- BERGES, J. A., AND P. G. FALKOWSKI. 1998. Physiological stress and cell death in marine phytoplankton: Induction of proteases in response to nitrogen or light limitation. *Limnol. Oceanogr.* **43**: 129–135, doi:10.4319/lo.1998.43.1.0129
- BIDLE, K. D., AND S. J. BENDER. 2008. Iron starvation and culture age activate metacaspases and programmed cell death in the marine diatom *Thalassiosira pseudonana*. *Eukaryot. Cell* **7**: 223–236, doi:10.1128/EC.00296-07
- , AND P. G. FALKOWSKI. 2004. Cell death in planktonic, photosynthetic microorganisms. *Nature Rev. Microbiol.* **2**: 643–655, doi:10.1038/nrmicro956
- BRUSSAARD, C. P. D., D. MARIE, R. THYRHAUG, AND G. BRATBAK. 2001. Flow cytometric analysis of phytoplankton viability following viral infection. *Aquat. Microb. Ecol.* **26**: 157–166, doi:10.3354/ame026157
- BUCCIARELLI, E., AND W. G. SUNDA. 2003. Influence of CO<sub>2</sub>, nitrate, phosphate, and silicate limitation on intracellular dimethylsulfoniopropionate in batch cultures of the coastal diatom *Thalassiosira pseudonana*. *Limnol. Oceanogr.* **48**: 2256–2265, doi:10.4319/lo.2003.48.6.2256
- CHARLSON, R. J., J. E. LOVELOCK, M. O. ANDREAE, AND S. G. WARREN. 1987. Oceanic phytoplankton, atmospheric sulfur, cloud albedo and climate. *Nature* **326**: 655–661, doi:10.1038/326655a0
- FALKOWSKI, P. G., R. T. BARBER, AND V. SMETACEK. 1998. Biogeochemical controls and feedbacks on ocean primary production. *Science* **281**: 200–206, doi:10.1126/science.281.5374.200
- FRADA, M., I. PROBERT, M. J. ALLEN, W. H. WILSON, AND C. DE VARGAS. 2008. The “Cheshire Cat” escape strategy of the coccolithophore *Emiliania huxleyi* in response to viral infection. *Proc. Natl. Acad. Sci. USA* **105**: 15944–15949, doi:10.1073/pnas.0807707105
- FRANKLIN, D. J., C. P. D. BRUSSAARD, AND J. A. BERGES. 2006. What is the role and nature of programmed cell death in microalgal ecology? *Eur. J. Phycol.* **41**: 1–41, doi:10.1080/09670260500505433
- GABRIC, A. J., P. A. MATRAL, R. P. KIENE, R. CROPP, J. W. H. DACEY, G. R. DiTULLIO, R. G. NAJJAR, R. SIMÓ, D. A. TOOLE, D. A. DEL VALLE, AND D. SLEZAK. 2008. Factors determining the vertical profile of dimethylsulfide in the Sargasso Sea during summer. *Deep-Sea Res. II* **55**: 1505–1518, doi:10.1016/j.dsr2.2008.02.002
- GARVEY, M., B. MORICEAU, AND U. PASSOW. 2007. Applicability of the FDA assay to determine the viability of marine phytoplankton under different environmental conditions. *Mar. Ecol. Prog. Ser.* **352**: 17–26, doi:10.3354/meps07134
- GEIDER, R. J., J. LAROCHE, R. M. GREENE, AND M. OLAIZOLA. 1993. Response of the photosynthetic apparatus of *Phaeodactylum tricorutum* (Bacillariophyceae) to nitrate, phosphate, or iron starvation. *J. Phycol.* **29**: 755–766, doi:10.1111/j.0022-3646.1993.00755.x
- HARADA, H., M. VILA-COSTA, J. CEBRIAN, AND R. P. KIENE. 2009. Effects of UV radiation and nitrate limitation on the production of biogenic sulfur compounds by marine phytoplankton. *Aquat. Bot.* **90**: 37–42, doi:10.1016/j.aquabot.2008.05.004

- HARRISON, P. J., R. E. WATERS, AND F. J. R. TAYLOR. 1980. A broad-spectrum artificial seawater medium for coastal and open ocean phytoplankton. *J. Phycol.* **16**: 28–35.
- HILDEBRAND, M., L. G. FRIGERI, AND A. K. DAVIS. 2007. Synchronized growth of *Thalassiosira pseudonana* (Bacillariophyceae) provides novel insights into cell-wall synthesis processes in relation to the cell cycle. *J. Phycol.* **43**: 730–740, doi:10.1111/j.1529-8817.2007.00361.x
- HYNNINEN, P. H., AND K. HYVÄRINEN. 2002. Tracing the allomerization pathways of chlorophylls by O<sup>18</sup>-labelling and mass spectrometry. *J. Org. Chem.* **67**: 4055–4061, doi:10.1021/jo010673f
- JEFFREY, S. W., AND G. M. HALLEGRAEFF. 1987. Chlorophyllase distribution in ten classes of phytoplankton: A problem for chlorophyll analysis. *Mar. Ecol. Prog. Ser.* **35**: 293–304, doi:10.3354/meps035293
- JIE, C., J. S. WALKER, AND B. J. KEELY. 2002. Atmospheric pressure chemical ionisation normal phase liquid chromatography mass spectrometry and tandem mass spectrometry of chlorophyll *a* allomers. *Rapid Commun. Mass Spectrom.* **16**: 473–479, doi:10.1002/rcm.597
- KELLER, M. D., W. K. BELLOW, AND R. R. L. GUILLARD. 1989. Dimethyl sulfide production in marine-phytoplankton. *Am. Chem. Soc. Symp. Ser.* **393**: 167–182.
- , AND W. KORJEFF-BELLOW. 1996. Physiological aspects of the production of dimethylsulfoniopropionate (DMSP) by marine phytoplankton, p. 131–142. *In* R. P. Kiene, P. T. Visscher, M. D. Keller, and G. O. Kirst [eds.], *Biological and environmental chemistry of DMSP and related sulfonium compounds*. Plenum Press, p. 131–142.
- KLIMOV, V. 2003. Discovery of phaeophytin function in the photosynthetic energy conversion as the primary electron acceptor of Photosystem II. *Photosynth. Res.* **76**: 247–253, doi:10.1023/A:1024990408747
- KROMKAMP, J., AND R. FORSTER. 2003. The use of fluorescence measurements in aquatic ecosystems: Differences between multiple and single turnover measuring protocols and suggested terminology. *Eur. J. Phycol.* **38**: 103–112, doi:10.1080/0967026031000094094
- LAKEMAN, M. B., P. VON DASSOW, AND R. A. CATTOLICO. 2009. The strain concept in phytoplankton ecology. *Harmful Algae* **8**: 746–758, doi:10.1016/j.hal.2008.11.011
- LAMKANFI, M., N. FESTJENS, W. DECLERCQ, T. VANDEN BERGHE, AND P. VANDENABEELE. 2007. Caspases in cell survival, proliferation and differentiation. *Cell Death Differ.* **14**: 44–55, doi:10.1038/sj.cdd.4402047
- LA ROCHE, J., R. J. GEIDER, L. M. GRAZIANO, H. MURRAY, AND K. LEWIS. 1993. Induction of specific proteins in eukaryotic algae grown under iron-deficient, phosphorus-deficient, or nitrogen-deficient conditions. *J. Phycol.* **29**: 767–777, doi:10.1111/j.0022-3646.1993.00767.x
- LEWIS, J., A. S. D. HARRIS, K. J. JONES, AND R. L. EDMONDS. 1999. Long-term survival of marine planktonic diatoms and dinoflagellates in stored sediment samples. *J. Plank. Res.* **51**: 343–354, doi:10.1093/plankt/21.2.343
- LOEBL, M., A. M. COCKSHUTT, D. A. CAMPBELL, AND Z. V. FINKEL. 2010. Physiological basis for high resistance to photoinhibition under nitrogen depletion in *Emiliania huxleyi*. *Limnol. Oceanogr.* **55**: 2150–2160, doi:10.4319/lo.2010.55.5.2150
- LOUDA, J. W., L. LIU, AND E. W. BAKER. 2002. Senescence and death related alteration of chlorophyll and carotenoids in marine phytoplankton. *Org. Geochem.* **33**: 1635–1653, doi:10.1016/S0146-6380(02)00106-7
- MARIE, D., N. SIMON, AND D. VAULOT. 2005. Phytoplankton cell counting by flow cytometry, p. 253–269. *In* R. A. Anderson [ed.], *Algal culturing techniques*. Elsevier Press, p. 253–269.
- NEBE-VON-CARON, G., P. J. STEPHENS, C. J. HEWITT, J. R. POWELL, AND R. A. BADLEY. 2000. Analysis of bacterial function by multi-colour fluorescence flow cytometry and single cell sorting. *J. Microbiol. Meth.* **42**: 97–114, doi:10.1016/S0167-7012(00)00181-0
- PEPERZAK, L., AND C. P. D. BRUSSAARD. 2011. Flow cytometric applicability of fluorescent vitality probes on phytoplankton. *J. Phycol.* **47**: 692–702, doi:10.1111/j.1529-8817.2011.00991.x
- PIRKER, H., C. PAUSZ, K. E. STODEREGGER, AND G. J. HERNDL. 2005. Simultaneous measurement of metabolic activity and membrane integrity in marine bacterioplankton determined by confocal laser-scanning microscopy. *Aquat. Microb. Ecol.* **39**: 225–233, doi:10.3354/ame039225
- RUDIGER, W. 2006. Biosynthesis of chlorophyll *a* and *b*: The last steps, *In* B. Grimm, R. J. Porra, W. Rudiger, and H. Scheer [eds.], *Chlorophylls and bacteriochlorophyll*, 25. Springer.
- SAUER, J., U. SCHREIBER, R. SCHMID, U. VOLKER, AND K. FORCHHAMMER. 2001. Nitrogen starvation-induced chlorosis in *Synechococcus* PCC 7942. Low-level photosynthesis as a mechanism of long-term survival. *Plant Physiol.* **126**: 233–243, doi:10.1104/pp.126.1.233
- SCHÄFER, H., N. MYRONOVA, AND R. BODEN. 2010. Microbial degradation of dimethylsulphide and related C-1-sulphur compounds: Organisms and pathways controlling fluxes of sulphur in the biosphere. *J. Exp. Bot.* **61**: 315–334, doi:10.1093/jxb/erp355
- SEGOVIA, M., AND J. A. BERGES. 2009. Inhibition of caspase-like activities prevents the appearance of reactive oxygen species and dark-induced apoptosis in the unicellular chlorophyte *Dunaliella tertiolecta*. *J. Phycol.* **45**: 1116–1126, doi:10.1111/j.1529-8817.2009.00733.x
- SIMÓ, R. 2001. Production of atmospheric sulfur by oceanic plankton: Biogeochemical, ecological and evolutionary links. *Trends Ecol. Evol.* **16**: 287–294, doi:10.1016/S0169-5347(01)02152-8
- SMITH, E. M., AND P. A. DEL GIORGIO. 2003. Low fractions of active bacteria in natural aquatic communities? *Aquat. Microb. Ecol.* **31**: 203–208, doi:10.3354/ame031203
- STEFELS, J. 2000. Physiological aspects of the production and conversion of DMSP in marine algae and higher plants. *J. Sea Res.* **43**: 183–197, doi:10.1016/S1385-1101(00)00030-7
- , M. STEINKE, S. TURNER, G. MALIN, AND S. BELVISO. 2007. Environmental constraints on the production and removal of the climatically active gas dimethylsulphide (DMS) and implications for ecosystem modelling. *Biogeochemistry* **83**: 245–275, doi:10.1007/s10533-007-9091-5
- STEINKE, M., G. MALIN, S. M. TURNER, AND P. LISS. 2000. Determinations of dimethylsulphoniopropionate (DMSP) lyase activity using headspace analysis of dimethylsulphide (DMS). *J. Sea Res.* **43**: 233–244, doi:10.1016/S1385-1101(00)00024-1
- SUNDA, W., D. J. KIEBER, R. P. KIENE, AND S. HUNTSMAN. 2002. An antioxidant function for DMSP and DMS in marine algae. *Nature* **418**: 317–320, doi:10.1038/nature00851
- SZYMCAK-ZYLA, M., G. KOWALEWSKA, AND J. W. LOUDA. 2008. The influence of microorganisms on chlorophyll *a* degradation in the marine environment. *Limnol. Oceanogr.* **53**: 851–862, doi:10.4319/lo.2008.53.2.0851
- TURNER, S. M., G. MALIN, L. E. BAGANDER, AND C. LECK. 1990. Interlaboratory calibration and sample analysis of dimethyl sulfide in water. *Mar. Chem.* **29**: 47–62, doi:10.1016/0304-4203(90)90005-W
- VELDHUIS, M. J. W., T. L. CUCCI, AND M. E. SIERACKI. 1997. Cellular DNA content of marine phytoplankton using two new fluorochromes: Taxonomic and ecological implications. *J. Phycol.* **33**: 527–541, doi:10.1111/j.0022-3646.1997.00527.x

- , G. W. KRAAY, AND K. R. TIMMERMANS. 2001. Cell death in phytoplankton: Correlation between changes in membrane permeability, photosynthetic activity, pigmentation and growth. *Eur. J. Phycol.* **36**: 167–177, doi:10.1080/09670260110001735318
- VERCAMMEN, D., W. DECLERCQ, P. VANDENABEELE, AND F. VAN BREUSEGEM. 2007. Are metacaspases caspases? *J. Cell Biol.* **179**: 375–380, doi:10.1083/jcb.200705193
- WALKER, J. S., AND B. J. KEELY. 2004. Distribution and significance of chlorophyll derivatives and oxidation products during the spring phytoplankton bloom in the Celtic Sea April 2002. *Org. Geochem.* **35**: 1289–1298, doi:10.1016/j.orggeochem.2004.06.017
- , A. H. SQUIER, D. H. HODGSON, AND B. J. KEELY. 2002. Origin and significance of <sup>13</sup>C-hydroxychlorophyll derivatives in sediments. *Org. Geochem.* **33**: 1667–1674, doi:10.1016/S0146-6380(02)00178-X

*Associate editor: Heidi M. Sosik*

*Received: 28 January 2011*

*Accepted: 26 September 2011*

*Amended: 07 November 2011*